

THE DESIGN OF THE IFUSP MAIN RACE-TRACK MICROTRON ACCELERATOR END MAGNETS

L. R. P. Kassab, FATEC, São Paulo, Brazil

J. Takahashi, M. N. Martins, P. Gouffon, IFUSP, São Paulo, Brazil

Abstract

This work deals with the design of the IFUSP main race-track microtron accelerator end magnets. This is the last stage of acceleration, composed of an accelerating section (1.04 m) and two end magnets (0.1585 T), in which a 5.10 MeV beam, produced by a race-track microtron booster, has its energy raised up to 31.15 MeV after 28 accelerations. Poisson code was used to give the final configuration that includes auxiliary pole pieces (clamps) and auxiliary homogenising gaps. The clamps avoid the beam vertical defocusing and the horizontal beam displacement produced by extended fringe fields (EFF); Ptrace code was used to perform the trajectory calculations in the fringe field region. The auxiliary homogenising gaps improve the field uniformity as they create a “magnetic shower” that provides uniformity of $\pm 0.3\%$ before the introduction of the correcting coils. The method of correction that employs correcting coils, used in the microtron booster magnets, enabled uniformity of $\pm 0.001\%$ in an average field of 0.1 T.

1 INTRODUCTION

Table 1 presents the parameters of the main race-track microtron accelerator. The machine operation is based on the resonance condition[1], $2\pi\Delta E/qBc^2 = \nu T_{RF}$ (ΔE is the energy gain, B is the magnetic field, c is the velocity of the light in the vacuum and ν is the multiple integer of the radiofrequency period T_{RF}) that determines, in first order, the magnetic field. This condition assumes that the magnetic field is uniform and, at the magnet edge, falls to zero abruptly (hard edge field). So these field requirements for the machine operation must be considered in the design of the end magnets whose field

Table 1: Parameters of the main race-track microtron

Injection energy (MeV)	5.10
Output energy (MeV)	31.15
Accelerating microwave (cm)	12.24
Energy gain per turn (MeV)	0.93
Total number of orbits	29
Radius of the first orbit (cm)	11.46
Radius of the last orbit (cm)	66.57
Magnetic Field (T)	0.1585
Average beam current (μA)	50
Distance between magnets (cm)	199.8

distributions have to enable the establishment of trajectories that are very near to the ideal ones. The end magnets incorporate homogenising air gaps and auxiliary pole pieces that were designed with the aid of Poisson. We should remark that, for the microtron booster end magnets[2], the calculations done with Poisson presented good agreement with the measurements. We also present the trajectory calculations, performed with Ptrace code, in which the effects of the extended fringe field[3] are compared with those of the reverse fringe field.

2 THE DESIGN OF THE END MAGNETS

The fundamental problem in end magnets design is to achieve high field uniformity, in an economical way, for a large ratio of gap depth to height. Two configurations are appropriate: C and half picture-frame (HPF) magnets. However, the HPF configuration is limited in field uniformity. This is manifested by the significant angle of the field lines with the perpendicular direction to the pole face in the iron-air interface. So for the end magnets of the main race-track microtron (Fig. 1) we

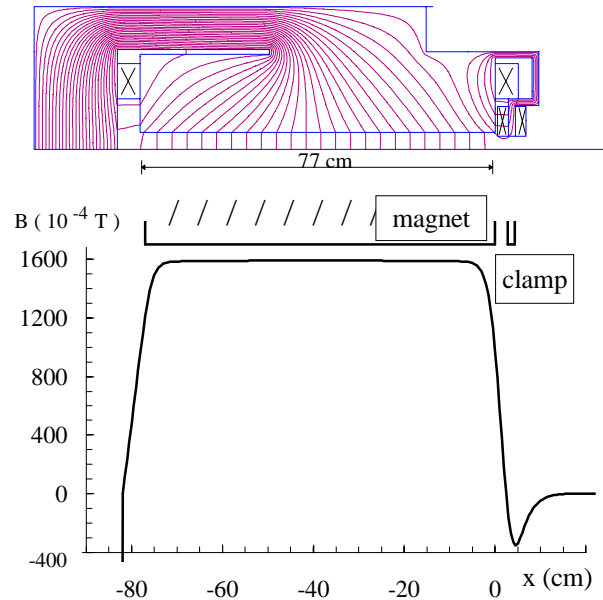


Figure 1: The main race-track microtron accelerator end magnets with the active clamp and the homogenising air gap; the magnetic field distribution in the middle plane, as a function of distance to the pole edge, calculated with Poisson.

decided for the C configuration, whose design was done with the aid of Poisson, a two dimensional program. The size of the magnets depends on the radius of the last orbit (66.6 cm). The end magnets were designed with height of 60 cm, rectangular pole pieces with $(77 \times 170) \text{ cm}^2$, gap height of 7 cm and weight of 4.10^4 N . The preliminary calculations revealed, for the magnetic field, variations of $\pm 0.4\%$, in the middle plane. However, to obtain this result, we had to increase the height of the magnets considerably (120 cm) and this would not represent an economical solution. The best one was found with a C configuration that includes homogenising air gaps, of 1cm, between the pole pieces and the yokes, and height reduced in 50% when compared to the other profile. The height of the magnets could be decreased because of the presence of the homogenising air gaps that provide uniformity of $\pm 0.3\%$ in the middle plane. For the same configuration, in the absence of the homogenising air gaps we would obtain for the magnetic field variations of $\pm 0.9\%$ in the middle plane. This result could only be optimised (considering the required uniformity of $\pm 0.01\%$ for this stage of acceleration) increasing the height of the magnets which is not a desirable solution. The position and the height of the homogenising gaps, that differs from the Purcell filters, usually inserted near the main gap, were also determined with Poisson code. The homogenising gaps deviate the field lines and create a “magnetic shower” (name given because of the field lines shape), improving the field uniformity and providing, in the horizontal middle plane of the magnet, a more uniform field distribution of $\pm 0.3\%$ before the introduction of the correcting coils. This method of correction, used in the microtron booster end magnets, enabled uniformity [4,5] of $\pm 0.001\%$, in an average field of 0.1 T, even when the current of operation was varied [6,7] up to $\pm 10\%$. The final configuration of the end magnets is shown in Fig. 1. The end magnets also incorporate auxiliary pole pieces (active clamps), with opposite excitation to that of the main poles, that provide a reverse fringe field region. These clamps avoid the effects caused by extended fringe fields (EFF) that compromise the machine operation: vertical defocusing and horizontal displacement of the beam. So, the reverse fringe field [8], as will be shown, avoids the vertical defocusing and reduces the horizontal displacement. Calculations with Poisson were necessary to adjust the profile of the clamps to a feasible configuration whose field distribution enables the particle acceleration. This was corroborated with Ptrace code that does numerical integration in the reverse fringe field region and calculates the trajectory and the energy of each orbit. Table 2 presents the coils parameters of the end magnets.

3 TRAJECTORY CALCULATIONS

Table 2: Coils parameters

	Main Coil	Auxiliary Coil
Wire diameter (mm)	7.010	2.946
Number of turns	70	198
Total current (A.turns)	5030	1640
Current (A)	71.8	8.3

The trajectory calculations show the effect of the reverse fringe field in the middle plane and in the ones situated out of it. Fig. 2 shows the trajectories of the first and last orbits, in the middle plane, in the presence of the extended and the reverse fringe fields. In both cases we observe beam displacements that are more significant for lower energies (3.36 cm for the first orbit and 0.52 cm for the last one).

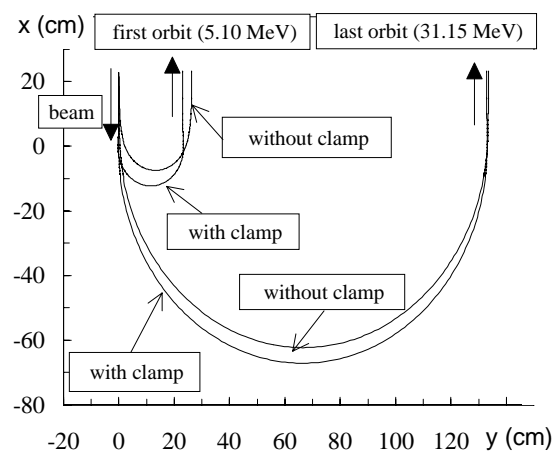


Figure 2: Trajectories in the presence of the EFF and the reverse fringe field, in the middle plane.

For the charged particle situated out of the middle plane, in the EFF, there are also vertical defocusing forces that move the particle away from the middle plane. The particle comes into the uniform region with a vertical velocity component, the orbit period is altered and the synchronism compromised. On the other hand, in the reverse fringe field region, the particle is submitted to weak vertical defocusing forces and maintain an almost constant distance from the middle plane. This is shown in Figs. 3, 4, and 5 that exhibit calculations for a particle that comes into the field 0.1 cm above the middle plane. In the EFF case, vertical displacements of 2 mm, for the first orbit, and of 0.2 mm, for the last one, are observed (Fig. 3). For the reverse fringe field, these vertical displacements are of $40 \mu\text{m}$ for the first orbit (Fig. 4) and of $4 \mu\text{m}$ for the last one (Fig. 5). Similar results were obtained for the microtron booster end magnets [2]. Table 3 presents the characteristics of some of the main race-track microtron orbits calculated with Ptrace code.

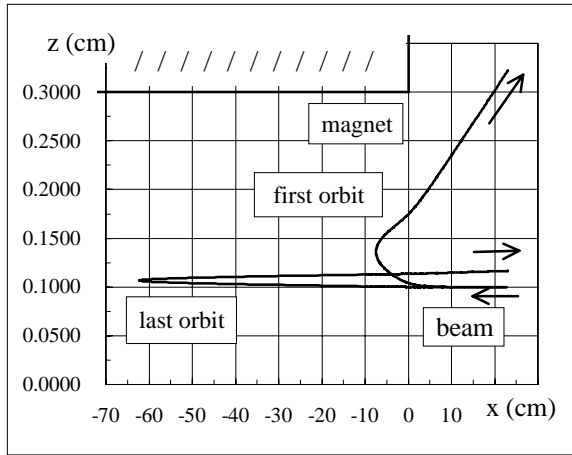


Figure 3: Trajectories of the first and the last orbits of a particle coming into the extended fringe field 0.1 cm above the middle plane.

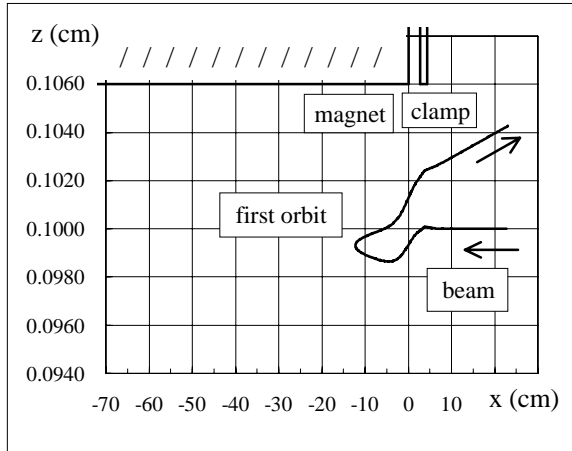


Figure 4: First orbit trajectory of a particle coming into the reverse fringe field 0.1 cm above the middle plane.

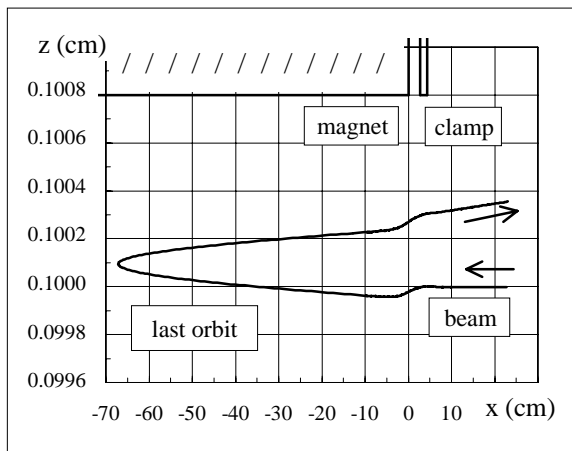


Figure 5: Last orbit trajectory of a particle coming into the reverse fringe field 0.1 cm above the middle plane.

Table 3: Radius and energy of the main race-track microtron orbits calculated with Ptrace

Orbit	Radius (cm)	Energy (MeV)
1	11.46	5.10
5	19.53	8.87
10	29.38	13.51
15	39.18	18.16
20	48.99	22.81
25	58.78	27.45
29	66.57	31.15

4 CONCLUSION

The simulations performed with Poisson and Ptrace codes show that the field distribution of the end magnets fulfil the requirements for the machine operation. The introduction of homogenising air gaps improved the uniformity of the magnetic field from $\pm 0.9\%$ to $\pm 0.3\%$. We should remark that there will probably appear inhomogeneities coming from material and mechanical problems. The introduction of correcting coils will then eliminate these problems. The active clamps were incorporated to avoid the effects caused by extended fringe fields. The horizontal displacements are reduced in about 3 cm, for the worst case. For the vertical movement, we observe maximum displacements of 40 μm , that is to say, weak vertical defocusing forces that maintain the trajectories very close to the middle plane.

5 ACKNOWLEDGMENTS

We would like to express our thanks to FATEC-SP for its encouragement during this work and to João A. de Lima, responsible for the construction of the race-track microtron booster end magnets in IFUSP, who gave suggestions concerning the mechanical problems of the main race-track microtron end magnets design. We also would like to thank the financial support from FAPESP.

REFERENCES

- [1] R.E. Rand, "Recirculating Electron Accelerators", Harwood Academic Publishers, New York, 1984.
- [2] L.R.P. Kassab et al., "Particle Accelerators", 59/2, 75, 1998.
- [3] H.A. Enge, "The Review of Scientific Instruments" 35, 278, 1964.
- [4] L.R.P. Kassab, P. Gouffon, M.N. Martins, "Nuclear Instruments and Methods" 404, 181, 1998.
- [5] L.R.P. Kassab, "Projeto, construção e teste do sistema de ímãs principais do acelerador microtron booster do IFUSP", Ph.D. thesis, Institute of Physics, University of São Paulo, 1996.
- [6] L.R.P. Kassab and P. Gouffon, "The use of correcting coils in end magnets of accelerators", PAC'97, Vancouver, May 1997.
- [7] L.R.P. Kassab and P. Gouffon, "Physical Review Special Topics - Accel. Beams" 1, 012401, 1998.
- [8] H. Babic and M. Sedlacek, "Nuclear Instruments and Methods" 56, 170, 1976.